# Dynamic Characterization of a Bioinspired Variable Stiffness Multi-Wingtip Device

Kyung Jun Lee<sup>a</sup> and Aimy Wissa<sup>a</sup>

<sup>a</sup>University of Illinois at Urbana-Champaign, 105 South Matthews Ave., Urbana, IL 61801

#### ABSTRACT

Birds are capable of performing complex maneuvers at low Reynolds numbers through the use of their feathers. The primary feathers, located towards the tip of a bird's wing, have shown to reduce the induced drag during flight. Inspired by the primary feathers, aircraft designers have implemented wingtips to increase aircraft efficiency and reduce induced drag. Previous researchers have mainly investigated static wingtips, which limits the use of such devices to a specific range of flight conditions. This research focuses on developing an adaptive multi-wingtip (AMW) device which yields improved aerodynamic efficiency (L/D ratio) across a wide range of angles of attack. This paper presents the initial steps in the design of the AMW device through the study and selection of suitable wingtip configurations. The design of the wingtip system is inspired by Harris's hawk. The key parameters in the design of the configurations are the dihedral angle, incidence angle, and gap space. Wind tunnel experiments of the wingtip configurations show that three wingtip configurations (planar no gap, planar 20 % gap, and non-planar 20 % Gap) are viable in yielding high aerodynamic efficiency and providing roll control across ranges of the angles of attack.

**Keywords:** Adaptive, Morphing, Wingtip, Winglet

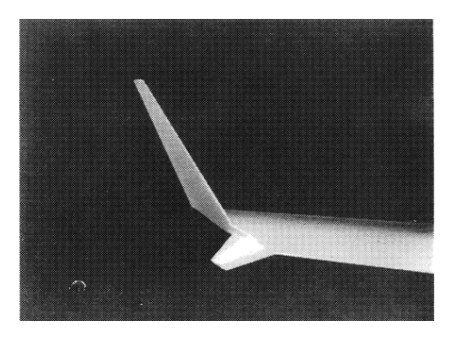
#### 1. INTRODUCTION

Birds are capable of performing complex maneuvers such as take-off, landing, cruising, and diving under various flight conditions<sup>1</sup>. Birds use their feathers during the flight to perform such complex maneuvers<sup>2</sup>. Among the feathers, the primary feathers, located at the tip of the wings, have been shown to reduce the induced drag<sup>3</sup>. Induced drag a is lift-independent drag that can account for up to 30 % of the total drag during cruising. Hence, reduction in the induced drag is desired for high efficiency<sup>4</sup>.

Inspired by the primary feathers, aircraft designers have implemented devices at the tip of the wing, named winglets, to reduce the induced drag of the aircraft. Winglets were first studied by Whitcomb. Wind tunnel experiments show an increase in the aerodynamic efficiency, defined as the lift to drag ratio, through the reduction in drag with the use of the winglets. In his experiments, Whitcomb compared the aerodynamic effects of adding winglets and extending the wingtip. The winglets reduced the induced drag by about 20 % and increased the lift-drag ratio by approximately 9 %, while the wingtip extension increased the lift to drag ratio by 4 % only. Hence, Whitcomb's study shows that the winglets improve the aerodynamic efficiency more than the wingtip extension with the same structural weight penalty<sup>5</sup>.

In addition to the traditional winglets that cover the entire chord of the base wing tip, researchers developed wingtip devices that partially cover the tip of the wing (Figure 1). Like the winglets, these wingtips, or wingtip sails as named by Spillman<sup>4</sup>, increase the aerodynamic efficiency by reducing induced drag. A recent study by Smith Et Al.<sup>6</sup> shows that multiple wingtips can be used to improve the L/D ratio when compared to traditional winglets.

Most of the previous studies that investigated the aerodynamic benefits of multiple wingtips have concluded that a single wingtip configuration can not improve L/D over the whole range of angles of attack<sup>4,5,6,7,8</sup>. At low angles of attack, a planar wingtip configuration reduces the induced drag the most (Figure 2). However, at high angles of attack, non-planar wingtip configurations reduce the induced drag more than planar configurations (Figure 2). A planar wingtip configuration is defined as a configuration where the wingtips chord lines are aligned with the base wing, while in a non-planar wingtip configuration, the plane of the wingtips is rotated with respect to the base wing chord line. Hence, to reduce the induced drag at both low and high angles of attack for



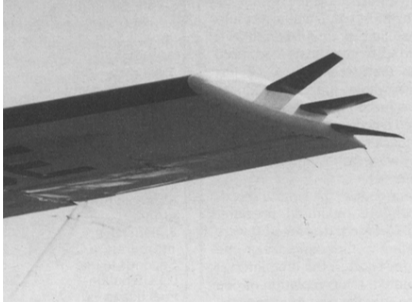
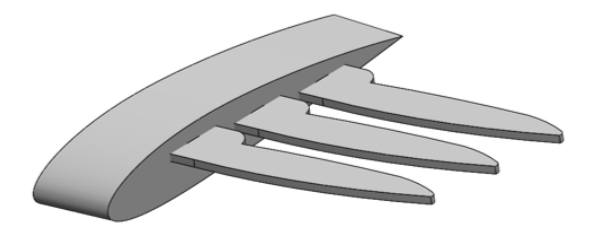


Figure 1. Winglet designed by Whitcomb<sup>5</sup> (Left). Wingtip sails designed by Spillman<sup>4</sup> (Right).

### **Planar Wingtip Configuration**

# Non-Planar Wingtip Configuration



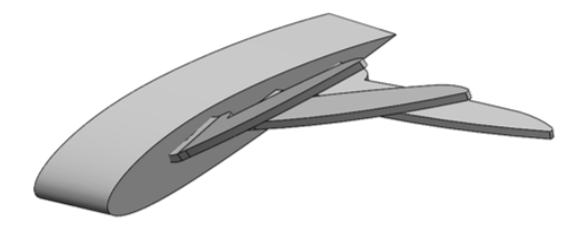


Figure 2. Visual representations of planar and non-planar wingtip configurations.

high efficiency, at least two different configurations are desired during flight, namely a planar and a non-planar wingtip configuration.

To achieve two, or more wingtip configurations, there is a need for an adaptive wingtip design that could improve efficiency at both low and high angles of attack. Therefore, this research focuses on developing an adaptive multi-wingtip (AMW) device which yields optimal aerodynamic efficiency (L/D ratio) across a wide range of angles of attack. However, before designing an adaptive wingtip system, the configurations of the wingtips suitable for the AMW device must first be identified and evaluated over a wide range of angles of attack. This paper presents the design and wind tunnel experimental evaluation of several wingtip configurations.

## 2. METHODS

### 2.1 Design of Wing and Wingtips

The design of the wing and wingtip system was inspired by Harris's hawks, a bird with slotted high lift wings (Figure 3). The Harris's hawk was selected as the source of inspiration because they share similar mission requirements as small scale unmanned aerial vehicles (UAVs). Both small-scale UAVs and Harris's hawk operate at low Reynolds number<sup>9</sup> and their wings both need to support payloads while requiring decent maneuverability <sup>10</sup>. Harris's hawks have slotted wingtips, which inspired the design of the wingtips presented in this paper.

First, inspired by the Harris' hawk, the base wing was designed with a moderate aspect ratio to support payloads while acquiring decent maneuverability. The wing has an aspect ratio of 4.63 (b = 312.5 mm,  $c_{ave} = 135$  mm), which falls within the wing aspect ratio range of birds with slotted high lift wings, namely between of  $4 - 6^2$ . The base wing has a taper ratio of 0.8 (i.e.,  $c_{root} = 150$  mm,  $c_{tip} = 120$  mm) similar to the design parameters given by Spillman<sup>4</sup>. An NACA 2414 airfoil, an airfoil commonly used for small-scale UAVs was used as the airfoil for the base wing. The NACA 2414 has low camber (max. 2 % at 39.6 % chord) and moderate thickness (max 14 % at 29.5 % chord)<sup>11</sup>.

The design of the wingtips was inspired by the Harris's hawks' primary feathers, shown in Figure 4. The slotting in the Harris' hawk wing is due to the emargination and notching shown near the tip of the feathers<sup>3</sup>.



Figure 3. Image of Harris's hawk during flight. The primary feathers are encircled in red.



Figure 4. Primary wing feather of birds. The region where emargination and notch exists is used as the design inspiration of the wingtips. Adapted from Feather Atlas<sup>12</sup>.

Therefore, the shape of the primary feather, especially in the region where the emargination and notch exists, was used as the design inspiration for the shape of the wingtips.

The dimensions of the wingtips were modeled after the design parameters by Spillman<sup>4</sup> and the image analysis of the wing and primary feathers of Harris's hawk. Spillman designed the chord of the wingtip  $(c_{wt})$  to be 16 % of the chord of the tip of the wing  $(c_{tip})$  (i.e.,  $c_{wt} = 0.16 \ c_{tip}$ ). The image analysis of Harris' hawk show that the chord of the wingtip  $(c_{wt})$  is 13 % of the chord of the root of the wing  $(c_{root})$  (i.e.,  $c_{wt} = 0.13 \ c_{root}$ ). For this design,the wingtip chord  $(c_{wt})$  of 19 mm and span  $(b_{wt})$  of 85 mm, respectively, which results in a  $c_{wt}/c_{tip} = 0.16$  and  $c_{wt}/c_{root} = 0.13$ . The overall dimensions of the designed wing and wingtips system are shown in Figure 5.

## 2.2 Key Parameters and Test Configurations

Both planar and non-planar wingtip configurations were tested in this study. The key parameters in the design of the wingtip configurations were the dihedral angle, incidence angle, and gap spacing, as shown in Figure 6. These key parameters were selected based on configurations in the literature that yielded improvements in the aerodynamic efficiency  $^{4,6,7,8,13}$ .

Dihedral angle is defined as the bending angle between the wingtip and the horizontal line of the wing (Figure 6, front view). Previous studies<sup>7,13</sup> show improvements in L/D ratio with a positive dihedral angle at the leading

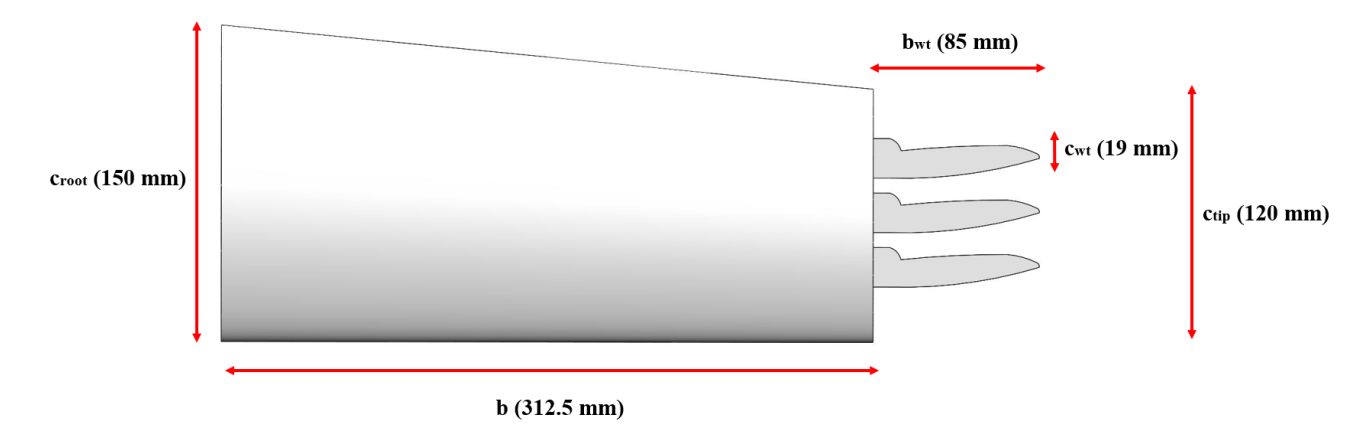


Figure 5. Dimensions of the designed wing and wingtips system.

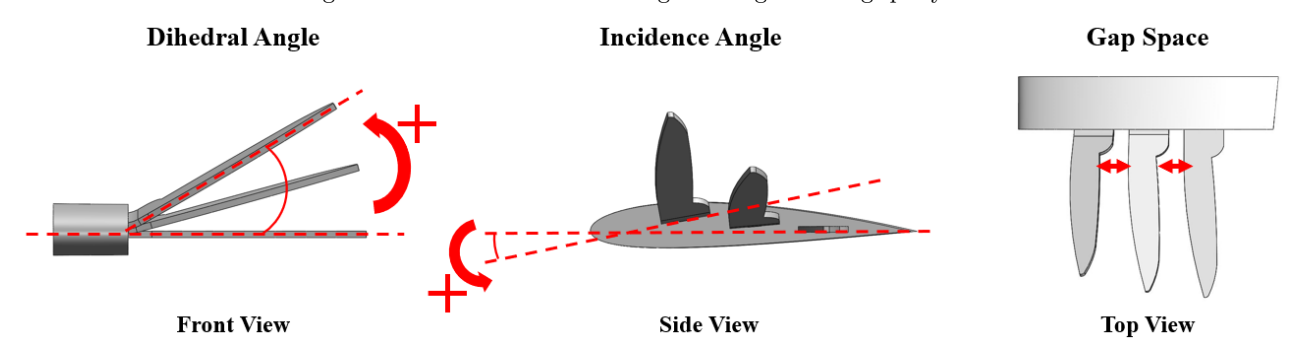


Figure 6. Key design parameters of the system. a) Dihedral angle: Bending angle between the wingtip and the horizontal line of the wing. b) Incidence angle: Twist angle between the wingtip and the chord line of the wing. c) Gap space: Total distance between the wingtips over the tip chord of the wing.

wingtip, cascading down to a zero dihedral angle for the trailing wingtip. The dihedral angles of  $30^{\circ}$  (leading),  $15^{\circ}$  (middle), and  $0^{\circ}$  (trailing) are tested in this study as this configuration yields the highest L/D ratio, as reported by Cerón-Muñoz and Catalano<sup>7</sup>.

Incidence angle is defined as the twist angle between the wingtip and the chord line of the wing (Figure 6, side view). Previous studies<sup>8,13</sup> show improvements in L/D ratio for a negative incidence angle at the leading wingtip, cascading up to a zero incidence angle at the trailing wingtip. The incidence angles of -10° (leading), -5° (middle), and 0° (trailing) are tested in this study as this configuration yields the greatest  $C_{L,max}$  amongst the wingtip configurations studied by Lynch Et Al<sup>8</sup>.

Gap space is defined as the total distance between the wingtips over the tip chord of the wing (Figure 6, top view). The gap space between the wingtips is measured from the notch to the emargination. Lynch Et Al.<sup>8</sup> shows improvements in  $C_{L,max}$  with the use of 20 % gap space between the wingtips. The effect of gap space on the wingtip configurations was tested without the gap (0 %) and with the gap (20 %).

A summary of the test configurations is shown in Figure 7. The baseline and tip extension were tested to compare the benefits of using the wingtip configurations. The wing tip extension has the same planform area as the sum of the area of the three wingtips. As previously presented by Gustafson Et Al. <sup>14</sup>, both the dihedral and incidence angles can be coupled using composite materials where the dihedral angle can induce an incidence angle. Thus, for these experiments, planar configurations (i.e., configurations with no dihedral), have zero incidence angles to simplify the actuation requirements for the AMW device.

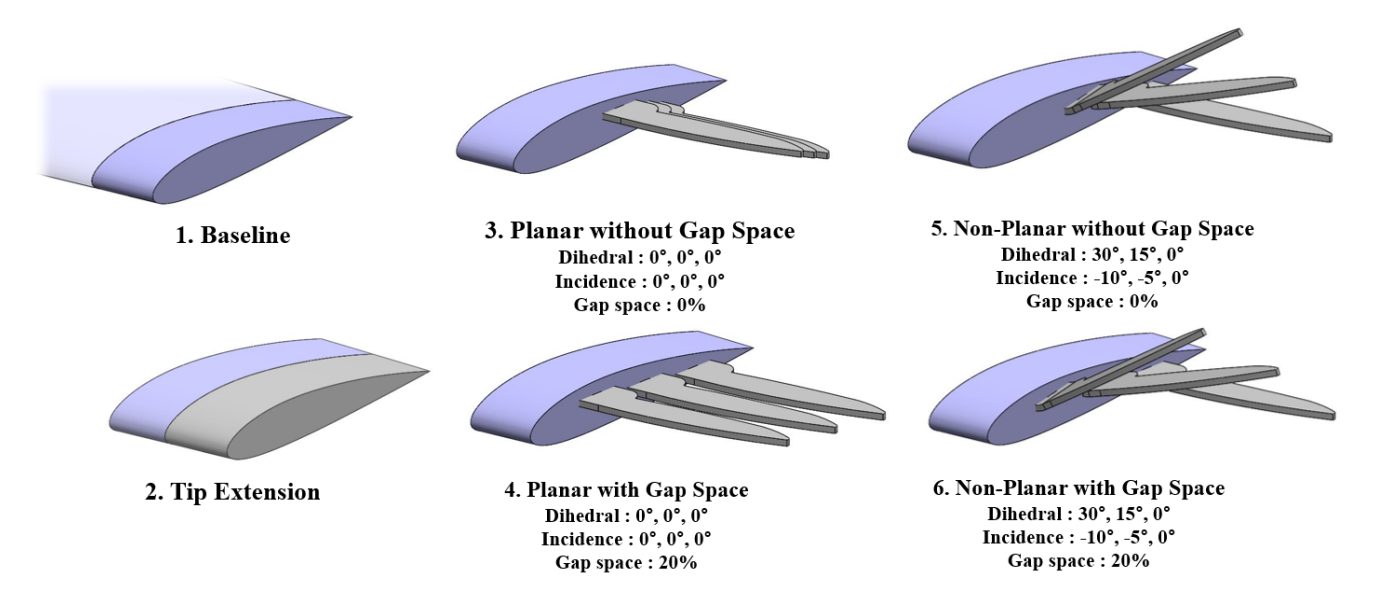


Figure 7. Summary of the test configurations. 1) Baseline. 2) Tip extension, which has the same planform area of the sum of the three wingtips. 3,4) Planar configuration with and without the gap space. 5,6) Non-planar configuration with and without the gap space.

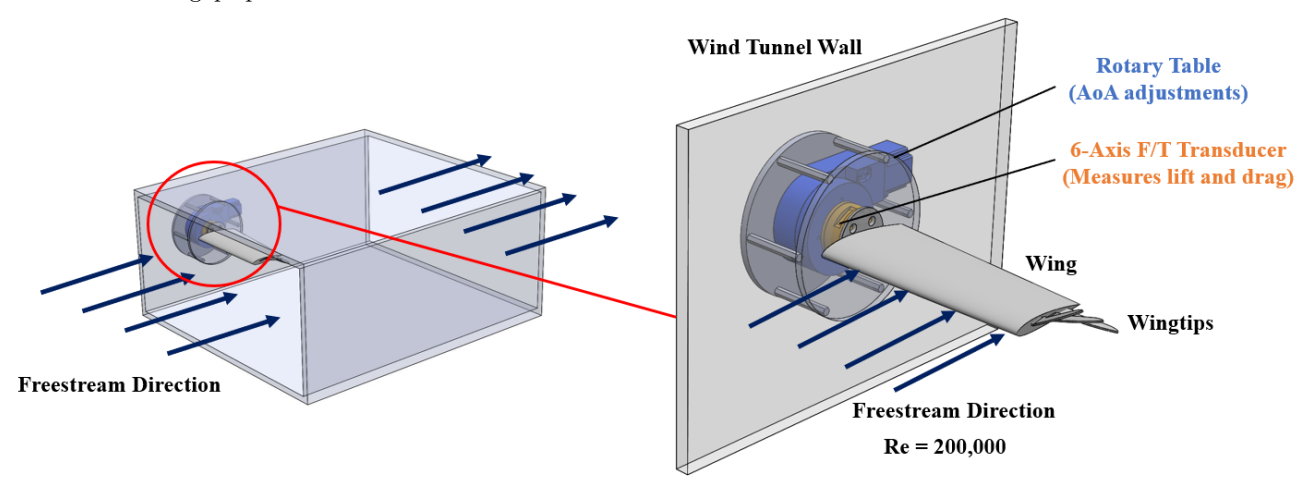


Figure 8. Schematic of the wind tunnel experiment setup. Velmex B48 rotary table is used for AoA adjustements and ATI Gamma 6-axis force/torque transducer is used for lift and drag measurements at Re = 200,000.

#### 2.3 Wind Tunnel Experiment

Wind tunnel experiments were conducted to answer:

- 1. Which wingtip configurations are suitable for maximizing the aerodynamic efficiency (L/D ratio) over a wide range of angles of attack?
- 2. How do the wingtip configurations perform compared to the baseline and the tip extension?
- 3. Are the wingtip configurations viable for roll control?

The experiments were performed at the wind tunnel facility located at the University of Illinois at Urbana-Champaign. The wind tunnel consists of four sections with the cross-section dimensions of 45 cm in length and 90 cm in height. The experiment ran at the foremost section of the wind tunnel to minimize turbulence. Wind speed was set to 23.0 m/s, which resulted in a Reynolds number of 200,000. The wind speed was measured and calibrated using a digital anemometer placed at the front of the wing. Details about the wind tunnel facilities and setup can be found in Reference<sup>15</sup>.

The wind tunnel experimental setup is shown in Figure 8. The system of the wing and wingtips was attached to the assembly of a rotary table and a 6-axis force/torque transducer. The assembly was placed at the sidewall of the wind tunnel. A Velmex B48 rotary table was used to perform an angle of attack sweep from -4° to 26°. An ATI Gamma 6-axis force/torque transducer was used to measure the forces acting on the wing. For each configuration and angle of attack, data was collected three times to account for measurement variation.

#### 3. RESULTS AND DISCUSSION

#### 3.1 Wingtip Configurations for High Efficiency

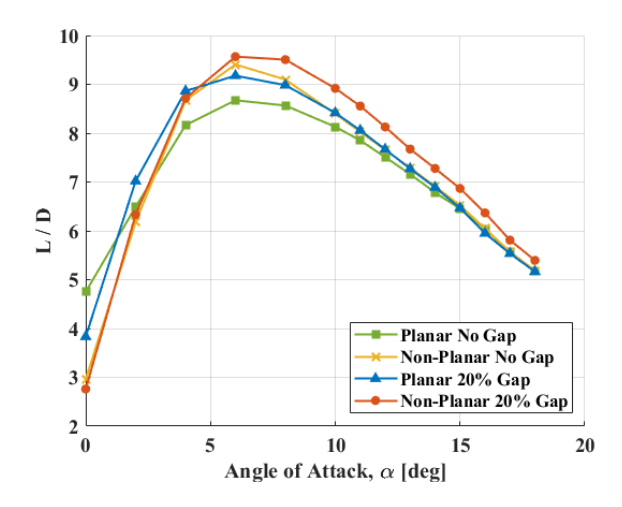


Figure 9. L/D results of the four wingtip configurations. At low angles of attack, planar 20 % gap configuration shows highest L/D ratio and at moderate to high angles of attack, non-planar 20 % gap configuration shows highest L/D ratio.

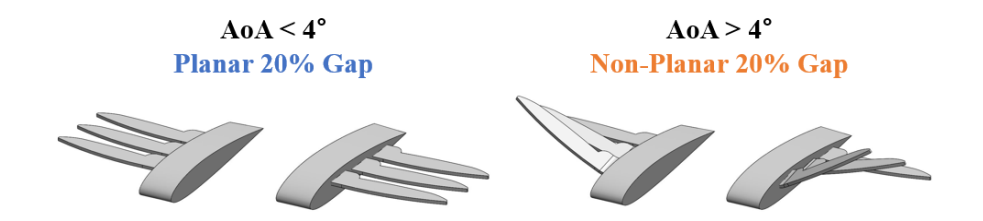


Figure 10. Summary of configurations for high efficiency at low (AoA  $< 4^{\circ}$ ) and moderate to high (AoA  $> 4^{\circ}$ ) angles of attacks.

The L/D results of the four wingtip configurations from angles of attack from  $0^{\circ}$  to  $18^{\circ}$  are shown in Figure 9. At low angles of attack (AoA <  $4^{\circ}$ ), the planar configuration with 20 % gap shows the highest L/D ratio. At moderate to high angles of attack (AoA >  $4^{\circ}$ ), the non-planar configuration with 20 % gap shows the highest L/D ratio. Therefore, to improve aerodynamic efficiency, the planar configuration with 20 % is needed at low AoA and the non-planar configuration with 20 % gap is needed at the moderate to high AoA, as shown in Figure 10.

The difference in aerodynamic efficiency is due to changes in lift rather than drag. Figure 11 shows the lift and drag results of the four wingtip configurations. The lift difference between the configurations is more notable

compared to the drag difference. Thus, in these experiments the wingtips configurations affect lift more than they affect drag.

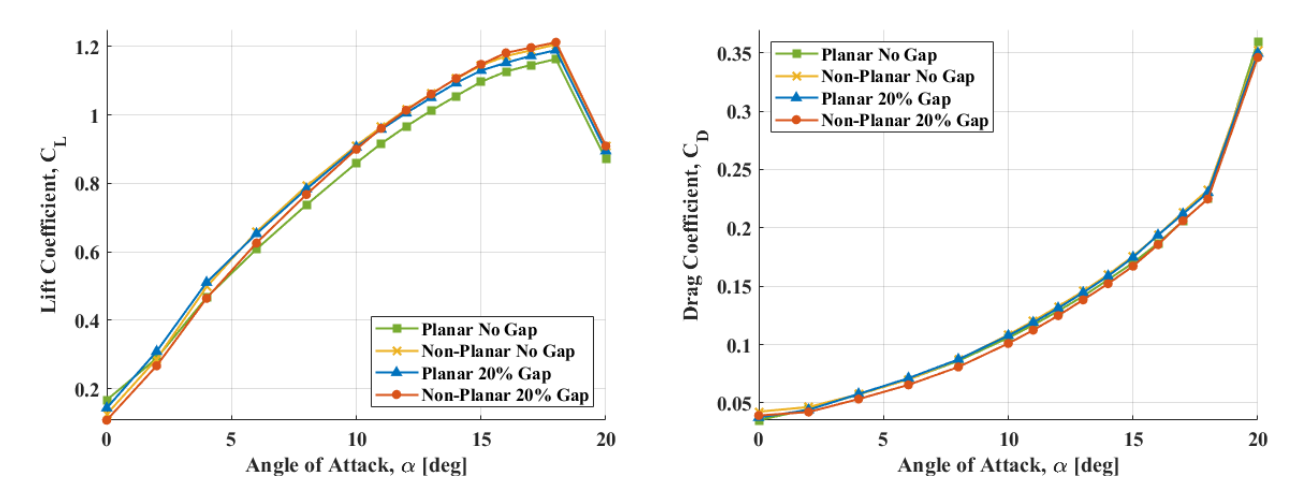


Figure 11. Lift (left) and drag (right) results of the four wingtip configurations. The lift difference is more notable compared to the drag difference between the configurations.

### 3.2 Comparison of the Wingtip Configurations with the Baseline and Tip Extension

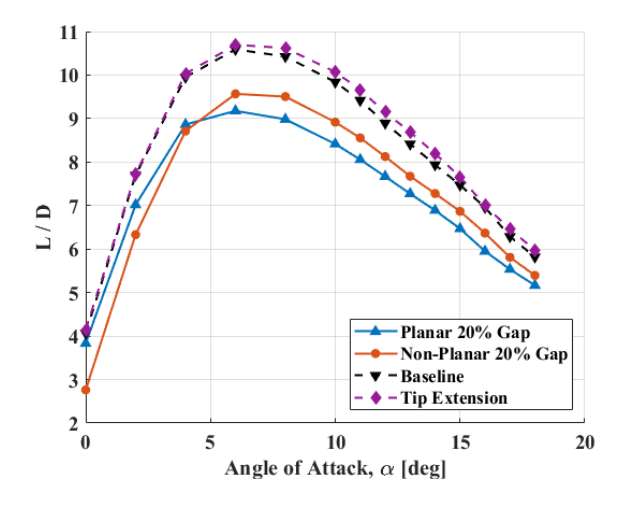


Figure 12. L/D results of the baseline, tip extension, and two wingtip configurations with the highest L/D ratio. The baseline and tip extension show higher L/D ratio compared to the wingtip configurations.

The L/D results of the baseline, tip extension, and two wingtip configurations that improve L/D the most, namely, the planar configuration with 20 % gap and non-planar configuration with 20 % gap configurations are shown in Figure 12. The results show that the two wingtip configurations yield a lower L/D ratio compared to the baseline and tip extension. Previous works of literature<sup>4,6,7,8</sup> show higher L/D ratio with the use of the wingtips compared to the baseline and the tip extension. However, the results from the experiment display the opposite.

Figure 13 shows the lift and drag results of the baseline, tip extension, and the two wingtip configurations. The low L/D ratio of the wingtip configurations mainly results from the drag forces. The wingtip configuration improve lift compared to the baseline. However, the same configurations result in a significant drag penalty. It is

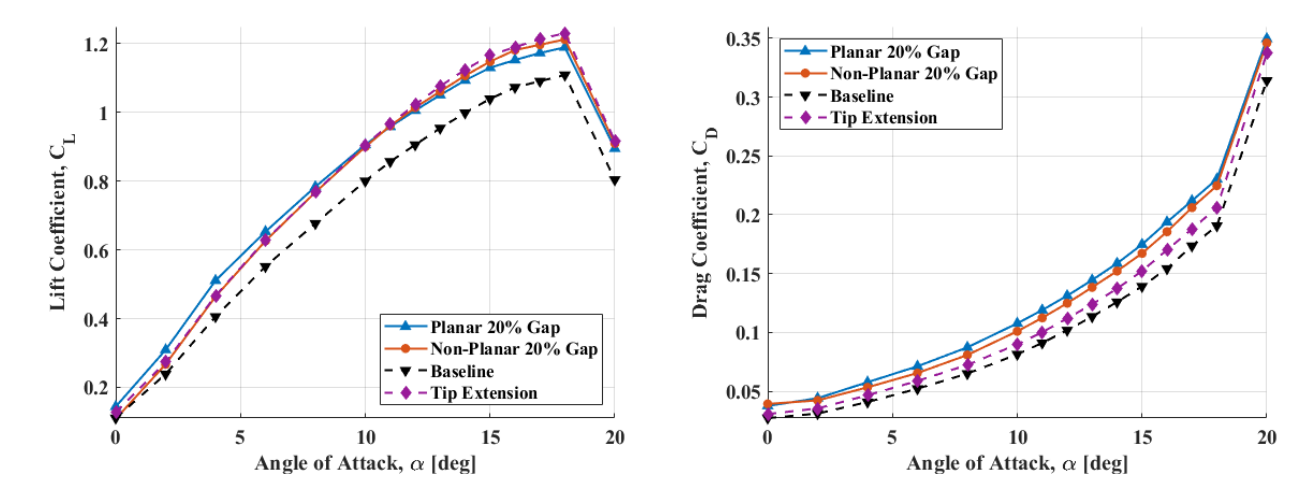


Figure 13. Lift (left) and drag (right) results of the baseline, tip extension, and two wingtip configurations with the highest L/D ratio. Low L/D ratio of the wingtip configurations mainly results from drag.

hypothesized that the drag penalty is due to the wingtip configurations' geometry. The wingtips has a flat plate cross-section, which is prone to stall. Hence, future work includes testing wingtips with airfoil-cross section.

The wingtips with airfoil cross-section may yield a higher L/D ratio compared to the baseline but not to the tip extension. The tip extension generates more lift compared to the wing with wingtips. Therefore, the tip extension may be more efficient compared to the baseline. However, there are advantages to using the wingtips over tip extension especially once the drag penalties are resolved. The wingtips are structurally lighter than the wingtip extension. Thus, adapting the configuration of the wingtips during flight is more feasible when compared to the wingtip extension. Moreover, when actuated asymmetrically, the wingtip configurations are viable as roll control effectors.

## 3.3 Wingtip Configurations for Roll Control

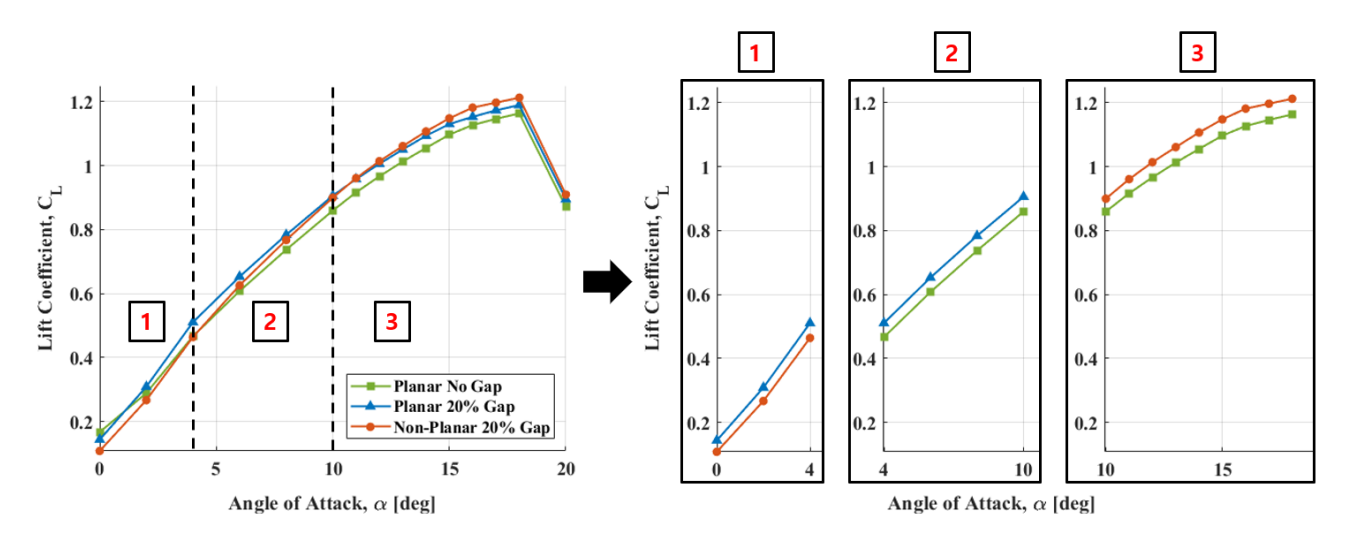


Figure 14. Lift results of the wingtip configurations for roll control. Numbers 1, 2, and 3 denotes three regions: low, moderate, and high angles of attack. The plot on the right shows simplified lift plot to observe three configurations viable for roll control.

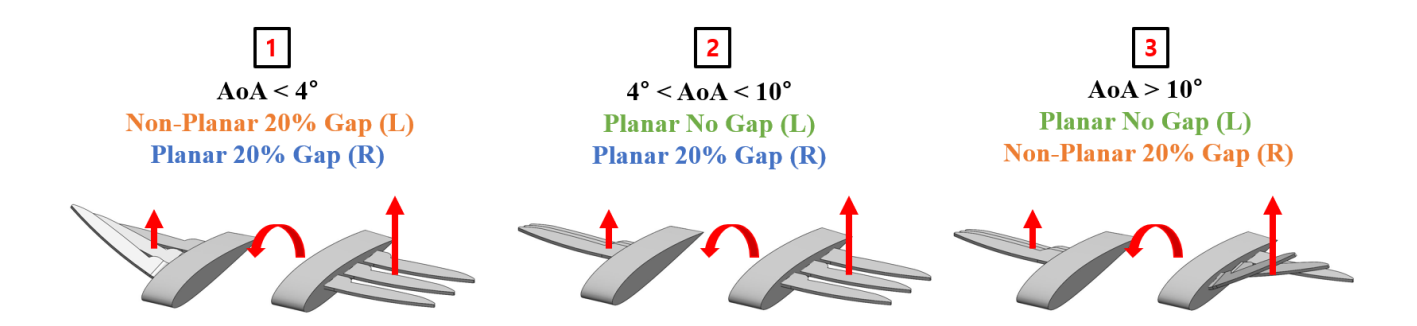


Figure 15. Summary of configurations for roll control at low (AoA <  $4^{\circ}$ ), moderate ( $4^{\circ}$  < AoA <  $10^{\circ}$ ), and high (AoA >  $10^{\circ}$ ) angles of attack.

Aside from the efficiency, the lift results from the experiment show the possibility of roll control due to the lift difference between the configurations (Figure 14). Different wingtip configurations can be used on the left and right wings to achieve a lift difference and create a rolling moment. At low angles of attack (AoA <  $4^{\circ}$ ), the non-planar 20 % gap and planar 20 % gap configurations can be used to create a relative lift difference of 19.5 %. At moderate angles of attack ( $4^{\circ}$  < AoA <  $10^{\circ}$ ), planar no gap and planar 20 % gap configurations can be used to create an average lift difference of 7.14 %. At high angles of attack (AoA >  $10^{\circ}$ ), planar no gap and non-planar 20 % gap configurations can be used to create an average lift difference of 4.53 %. Hence, adapting the shape of the wingtips between three wingtip configurations namely, non-planar 20 % gap, planar 20 % gap, and planar no gap configurations can be used to generate a rolling moment across a wide range of angles of attack. (Figure 15).

#### 4. CONCLUSION AND FUTURE WORK

In this paper, wind tunnel experiments show the feasibility of using wingtip devices to achieve high aerodynamic efficiency and roll control. The efficiency of the wingtips is lower than that of the tip extension in terms of L/D. However, the benefits of using the wingtips over the tip extension exist. The wingtips generate lift close to that of the tip extension with a lighter structural weight. Additionally, asymmetric actuation of the wingtips devices can achieve roll control over a wide range of angles of attack.

For future work, wind tunnel experiments of the wingtip configurations with an airfoil cross-section wingtips are required to mitigate the drag penalty. Based on these updated experimental results, we will select the feasible configurations for the AMW device and design the actuation strategy needed to achieve both high aerodynamic efficiency and roll control.

#### ACKNOWLEDGMENTS

The initial stages this work was partly funded through the Air Force Summer Faculty Fellowship Program. Kyung Jun Lee was supported on a fellowship from the University of Illinois at Urbana-Champaign Mechanical Science and Engineering Department.

## REFERENCES

- [1] Tobalske, B. W., "Biomechanics and physiology of gait selection in flying birds," in [*Physiological and Biochemical Zoology*], **73**(6), 736–750 (2000).
- [2] Taylor, G. K., Carruthers, A. C., Hubel, T. Y., and Walker, S. M., "Wing Morphing in Insects, Birds and Bats: Mechanism and Function," in [Morphing Aerospace Vehicles and Structures], 11–40, John Wiley Sons, Ltd, Chichester, UK (mar 2012).
- [3] Tucker, V. A., "GLIDING BIRDS: REDUCTION OF INDUCED DRAG BY WING TIP SLOTS BETWEEN THE PRIMARY FEATHERS," Journal of Experimental Biology 180(1), 285–310 (1993).

- [4] Spillman, J. J., "USE OF WING TIP SAILS TO REDUCE VORTEX DRAG.," Aeronaut J 82(813), 387–395 (1978).
- [5] Whitcomb, R. T., "A design approach and selected wind tunnel results at high subsonic speeds for wing-tip mounted winglets," Nasa Tn D-8260 (July), 1–33 (1976).
- [6] Smith, M. J., Komerath, N., Ames, R., Wong, O., and Pearson, J., "Performance analysis of a wing with multiple winglets," in [19th AIAA Applied Aerodynamics Conference], American Institute of Aeronautics and Astronautics Inc. (2001).
- [7] Cerón-Muñoz, H. D. and Catalano, F. M., "Experimental analysis of the aerodynamic characteristics adaptive of multi-winglets," *Proceedings of the Institution of Mechanical Engineers, Part G: Journal of Aerospace Engineering* **220**(3), 209–215 (2006).
- [8] Lynch, M., Mandadzhiev, B., and Wissa, A., "Bioinspired wingtip devices: A pathway to improve aerodynamic performance during low Reynolds number flight," *Bioinspiration and Biomimetics* 13, 036003 (mar 2018).
- [9] WITHERS, P. C., "An Aerodynamic Analysis of Bird Wings as Fixed Aerofoils," Journal of Experimental Biology 90(1), 143-162 (1981).
- [10] Savile, D. B. O., "Adaptive Evolution in the Avian Wing," Evolution 11, 212 (jun 1957).
- [11] Selig, M., Guglielmo, J. J., Broeren, A. P., and Giguere, P., "Summary of Low-Speed Airfoil Data Summary of Low-Speed Airfoil Data," 1, 315 (1995).
- [12] U.S. Fish and Wildlife Service, "The Feather Atlas Feather Identification and Scans U.S. Fish and Wildlife Service Forensics Laboratory," (2010).
- [13] Spillman, J. J. and McVitie, A. M., "WING TIP SAILS WHICH GIVE LOWER DRAG AT ALL NORMAL FLIGHT SPEEDS.," *Aeronautical Journal* 88(878), 362–369 (1984).
- [14] Gustafson, K., Urrutia, L., Pankonien, A., Reich, G., and Wissa, A., "Adaptive and compliant wingtip devices enabled by additive manufacturing and multistable structures," in [Bioinspiration, Biomimetics, and Bioreplication IX], Lakhtakia, A., Martín-Palma, R. J., and Knez, M., eds., 10965, 18, SPIE (mar 2019).
- [15] Ito, M. R., Duan, C., and Wissa, A. A., "The function of the alula on engineered wings: A detailed experimental investigation of a bioinspired leading-edge device," *Bioinspiration and Biomimetics* **14**, 056015 (aug 2019).